J|A|C|S ARTICLES

Published on Web 08/11/2009

No Confinement Needed: Observation of a Metastable Hydrophobic Wetting Two-Layer Ice on Graphene

Greg A. Kimmel,*,† Jesper Matthiesen,† Marcel Baer,‡ Christopher J. Mundy,*,† Nikolay G. Petrik,† R. Scott Smith,† Zdenek Dohnálek,† and Bruce D. Kay*,†

Chemical and Materials Sciences Division, Pacific Northwest National Laboratory, P.O. Box 999, Richland, Washington 99352, and Lehrstuhl für Theoretische Chemie, Ruhr-Universität Bochum, 44780 Bochum, Germany

Received June 9, 2009; E-mail: gregory.kimmel@pnl.gov; bruce.kay@pnl.gov; chris.mundy@pnl.gov

Abstract: The structure of water at interfaces is crucial for processes ranging from photocatalysis to protein folding. Here, we investigate the structure and lattice dynamics of two-layer crystalline ice films grown on a hydrophobic substrate, graphene on Pt(111), with low energy electron diffraction, reflection−absorption infrared spectroscopy, rare-gas adsorption/desorption, and ab initio molecular dynamics. Unlike hexagonal ice, which consists of stacks of *puckered* hexagonal "bilayers", this new ice polymorph consists of two *flat* hexagonal sheets of water molecules in which the hexagons in each sheet are stacked directly on top of each other. Such two-layer ices have been predicted for water confined between hydrophobic walls, but not previously observed experimentally. Our results show that the two-layer ice forms even at zero pressure at a single hydrophobic interface by maximizing the number of hydrogen bonds at the expense of adopting a nontetrahedral geometry with weakened hydrogen bonds.

1. Introduction

The structure of water at interfaces is crucial in areas as diverse as protein folding,[1−3] the structure of living cells,[2] and heterogeneous catalysis.[4] Water's interactions at interfaces span the range from strongly hydrophobic to strongly hydrophilic. For hydrophilic substrates, it is obvious that the strong binding of the water to the substrate can influence the structure of the water film near the substrate. However, even very hydrophobic substrates can have a profound influence on the structure of water in the vicinity because of the tendency for substrates to induce stratification in the water near the interface.[5−8] The lack of bonding to a hydrophobic substrate, in conjunction with the stratification, can lead to significant distortions away from ice's preferred tetrahedral bonding geometry. For example, molecular dynamics (MD) simulations have predicted the existence of quasi-two-dimensional crystalline and amorphous ices between planar hydrophobic walls, which have distinctive properties such as nontetrahedral bonding geometries, novel phase transitions and anomalous self-diffusion.[6−10] To date, these structures have not been observed experimentally. A closely related topic, the structure and dynamics of water confined in nonplanar geometries such as carbon nanotubes, is also of great current interest.[8,11,12]

Here we report the experimental observation of a metastable, quasi-two-dimensional crystalline ice grown on a planar hydrophobic substrate, graphene on Pt(111), with a unique, nontetrahedral bonding geometry. This new ice polymorph consists of two *flat* hexagonal sheets of water molecules in which the hexagons in each sheet are stacked directly on top of each other. Each molecule forms three hydrogen bonds with its neighbors within a given layer with oxygen−oxygen−oxygen bond angles, θ_{OOO}, of 120° and a fourth hydrogen bond with a molecule in the other sheet, with $\theta_{OOO} = 90°$. In this arrangement, the number of hydrogen bonds is maximized and there are no dangling OH's or lone pair electrons on either surface of the ice film (i.e., these ice surfaces are expected to be hydrophobic). The two-layer ice, which grows at low temperatures (∼100−135 K), has been characterized experimentally with low energy electron diffraction (LEED), reflection−absorption infrared spectroscopy (RAIRS), and rare-gas temperature programmed desorption (TPD), and theoretically with ab initio MD simulations. The results presented here lend support to the previous simulations predicting the existence of two-layer ices in the confined hydrophobic geometries that are relevant to protein folding. Furthermore, the unusual bonding geometry exhibited in the two-layer ice may also play a role in liquid water at hydrophobic interfaces.

The properties of water at well-charaterized planar surfaces (such as metal and metal oxide single crystals) have been

† Pacific Northwest National Laboratory.
‡ Ruhr-Universität Bochum.

(1) Kauzmann, W. *Adv. Protein Chem.* **1959**, *14*, 1.
(2) Tanford, C. *Science* **1978**, *200*, 1012.
(3) Chandler, D. *Nature* **2005**, *437*, 640.
(4) Henderson, M. A. *Surf. Sci. Rep.* **2002**, *46*, 1.
(5) Lee, C. Y.; McCammon, J. A.; Rossky, P. J. *J. Chem. Phys.* **1984**, *80*, 4448.
(6) Zangi, R. *J. Phys.: Condens. Matter* **2004**, *16*, S5371.
(7) Giovambattista, N.; Rossky, P. J.; Debenedetti, P. G. *Phys. Rev. Lett.* **2009**, *102*, 050603.
(8) Cicero, G.; Grossman, J. C.; Schwegler, E.; Gygi, F.; Galli, G. *J. Am. Chem. Soc.* **2008**, *130*, 1871.
(9) Koga, K.; Tanaka, H.; Zeng, X. C. *Nature* **2000**, *408*, 564.
(10) Koga, K.; Zeng, X. C.; Tanaka, H. *Phys. Rev. Lett.* **1997**, *79*, 5262.
(11) Byl, O.; Liu, J. C.; Wang, Y.; Yim, W. L.; Johnson, J. K.; Yates, J. T. *J. Am. Chem. Soc.* **2006**, *128*, 12090.
(12) Wang, H. J.; Xi, X. K.; Kleinhammes, A.; Wu, Y. *Science* **2008**, *322*, 80.

 10.1021/ja904708f CCC: $40.75

extensively studied using surface science techniques.[4] Although most of these studies have explored hydrophilic surfaces, the adsorption, desorption, and growth kinetics of thin water films on hydrophobic surfaces such as graphite[13−15] and hydrocarbons[16] have also been reported. On such surfaces, water monomers interact weakly, and at temperatures above ∼100 K water condensation typically requires the nucleation of small clusters.[14,16] However, water films on these surfaces have not been investigated with techniques that are sensitive to the structure, or have been investigated at lower temperatures where amorphous films are formed.

2. Methods

Experiment. The experiments were carried out in two ultrahigh vacuum systems which have been described previously.[17,18] Both systems were equipped with a closed-cycle helium cryostat (Advanced Research Systems CSW 204B), a molecular beamline for dosing adsorbates, a Fourier transform infrared spectrometer (Bruker Vertex 70 or Bruker Equinox 55) and a quadrupole mass spectrometer (Extrel). One system[18] also had a low-energy electron diffraction (LEED) spectrometer (Princeton Research Instruments) and an Auger electron spectrometer (Perkin-Elmer). Typical base pressures for the systems were $\sim 8 \times 10^{-11}$ Torr. The polished platinum single crystals (Princeton Scientific Corp.) were 10 mm in diameter, 1 mm thick, and were cut to within ±0.5° of the (111) surface orientation. The samples were resistively heated, and the temperatures were measured with a K-type thermocouple spot-welded to rear side of the samples. One Pt(111) sample was cleaned with cycles of neon ion sputtering (2 keV) and annealing at 1050 K in vacuum. The second sample was cleaned by neon ion sputtering (1 keV), followed by annealing in oxygen (7×10^{-7} Torr) at 900 K and then in vacuum at 1200 K. (The results presented did not depend on which cleaning procedure was used.)

Graphene films were prepared by exposing the Pt(111) samples to decane at high temperatures (1000−1200 K). This procedure produces a single layer of carbon with the structure of graphite, which grows in islands on the Pt(111).[19,20] Thin films of H_2O or D_2O were deposited on the substrate at temperatures ranging from 20 to 152 K. Water coverages, θ, are defined in terms of the density of water molecules in the (0001) plane of hexagonal ice (I_h): 1 ML $\equiv 1.14 \times 10^{15}$ molecules/cm^2.[21] For incident water fluxes of ∼0.2 ML/s and temperatures below ∼100 K, the resulting films were amorphous, while for temperatures above ∼140 K nonwetting, three-dimensional ices were formed. However, for temperatures between ∼100 K and ∼135 K, the water initially grew in ordered islands that were two molecular layers thick. The graphene films were stable under electron irradiation by the energetic electrons during LEED. However, the LEED patterns observed for the water films typically disappeared after several seconds exposure (for electron beam currents of ∼1−3 μA), presumably because of efficient sputtering by the electrons.[22]

Theory. Two-layer ice films were investigated with ab initio MD using density functional theory (DFT) in conjunction with pseudopotentials as implemented in the CP2K software suite.[23] The initial configuration for our simulations consisted of two flat hexagonal sheets, each with 24 water molecules, stacked directly above or below each other in a supercell. The starting geometries were chosen from classical MD simulations of two-layer ices confined between hydrophobic walls.[7,10] However, for our simulations, there are no hydrophobic walls. (Recall that experimentally, the two-layer ices are deposited on a single, planar hydrophobic surface.) The calculations were performed with a time-step of 0.5 fs. The supercell dimensions (1.6500 nm × 1.4289 nm, and 2.0000 nm normal to the two-layer ice) were initially determined from semiempirical calculations using the density functional tight binding model[24] and self-consistently checked using DFT. The ab initio MD simulations utilized Becke exchange and the Lee−Yang−Parr correlation functional (BLYP) in conjunction with a TZV2P basis set for the orbitals and Goedecker−Teter−Hutter (GTH) pseudopotentials.[25] The energy cutoff was 280 Ry. Infrared (IR) spectra were computed by Fourier transforming the dipole autocorrelation function, where the dipole was computed using the Berry-phase formulation for periodic systems.[26] The final IR spectra were smoothed with a Gaussian with a width of 10 cm^{-1}.

3. Results and Discussion

We used LEED to characterize the thin water films that grow on graphene/Pt(111). A LEED pattern directly reveals the symmetry of the surface, and the lattice constant (parallel to the surface) can also be obtained.[27] Figure 1a shows a typical LEED pattern for graphene on Pt(111) for an incident electron energy, E_i, of 133.1 eV. The 6 sharp spots inside the segmented ring are the first order diffraction peaks from Pt(111). The segmented ring is due to the graphene that grows in a mosaic of domains on Pt(111).[19,20] Within each domain, the graphene has the same lattice constant ($a_{gr} = 0.246$ nm), but the domains grow in several different rotated, epitaxial phases leading to the observed pattern.

Figure 1b shows the LEED pattern at $E_i = 21.4$ eV for a 2 ML H_2O film deposited at 125 K on graphene/Pt(111). Similar patterns are obtained for other coverages ($0 < \theta < 2$ ML), a range of growth temperatures, and also for D_2O (see Figure 1c). The LEED patterns for these water films, which form segmented rings similar to the graphene films, provide several important pieces of information. First, the pattern indicates that the water film is ordered, i.e., this is a *crystalline* ice film. Furthermore, this ice film has the same hexagonal symmetry as the graphene substrate on which it grows, and the water film is rotationally aligned with graphene despite the weak interaction between the water film and the graphene. The lattice constant for this 2 ML ice film is $a_{2D} = 0.481$ nm ± 0.003 nm in the plane parallel to the surface. For comparison, the lattice constant, a_{I_h}, in the (0001) plane for I_h at 25 K is $a_{I_h} = 0.450$ nm.[21] Thus, the ice films grown on graphene/Pt(111) have an in-plane lattice constant that is 6.4% larger than the constant for I_h.

To assess the accuracy of the lattice parameter obtained experimentally for the planar, two-layer ice with the LEED spectrometer, we also investigated multilayer cubic ice (I_c) films

(13) Chakarov, D. V.; Osterlund, L.; Kasemo, B. *Vacuum* **1995**, *46*, 1109.
(14) Andersson, P. U.; Suter, M. T.; Markovic, N.; Pettersson, J. B. C. *J. Phys. Chem. C* **2007**, *111*, 15258.
(15) Sanfelix, P. C.; Holloway, S.; Kolasinski, K. W.; Darling, G. R. *Surf. Sci.* **2003**, *532*, 166.
(16) Linderoth, T. R.; Zhdanov, V. P.; Kasemo, B. *Phys. Rev. Lett.* **2003**, *90*, 156103.
(17) Petrik, N. G.; Kimmel, G. A. *J. Chem. Phys.* **2004**, *121*, 3736.
(18) Zubkov, T.; Smith, R. S.; Engstrom, T. R.; Kay, B. D. *J. Chem. Phys.* **2007**, *127*, 184707.
(19) Enachescu, M.; Schleef, D.; Ogletree, D. F.; Salmeron, M. *Phys. Rev. B* **1999**, *60*, 16913.
(20) Ueta, H.; Saida, M.; Nakai, C.; Yamada, Y.; Sasaki, M.; Yamamoto, S. *Surf. Sci.* **2004**, *560*, 183.
(21) Petrenko, V. F.; Whitworth, R. W. *Physics of Ice*; Oxford University Press: Oxford, U.K., 1999.
(22) Petrik, N. G.; Kimmel, G. A. *J. Chem. Phys.* **2005**, *123*, 054702.
(23) The CP2K developers group, 2000−2009, http://cp2k.berlios.de
(24) Frauenheim, T.; Seifert, G.; Elstner, M.; Hajnal, Z.; Jungnickel, G.; Porezag, D.; Suhai, S.; Scholz, R. *Phys. Status Solidi B* **2000**, *217*, 41.
(25) Goedecker, S.; Teter, M.; Hutter, J. *Phys. Rev. B* **1996**, *54*, 1703.
(26) Silvestrelli, P. L.; Bernasconi, M.; Parrinello, M. *Chem. Phys. Lett.* **1997**, *277*, 478.
(27) Heinz, K. *Rep. Prog. Phys.* **1995**, *58*, 637.

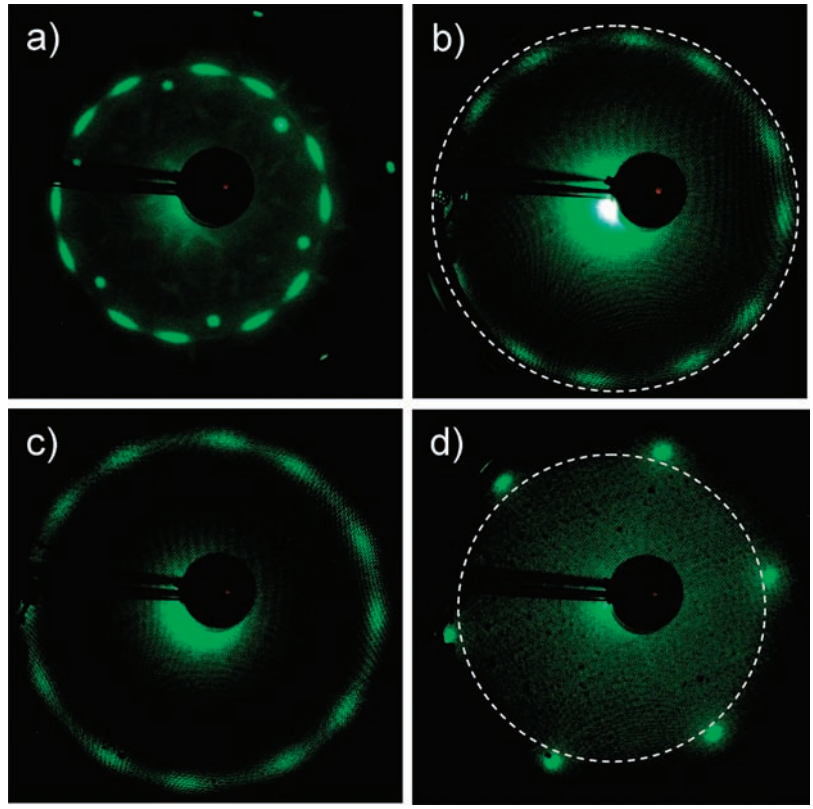

Figure 1. Low-energy electron diffraction (LEED) patterns for a) graphene/Pt(111) with $E_i = 133.1$ eV, (b) 2 ML H_2O deposited at 125 K on graphene/Pt(111) with $E_i = 21.4$ eV, (c) 2 ML D_2O deposited at 125 K on graphene/Pt(111) with $E_i = 20.5$ eV, and (d) 20 ML H_2O deposited at 145 K on Pt(111). The dashed white line in b shows the expected position for the first order diffraction spots if the lattice constant was 0.450 nm (corresponding to I_h). The dashed white line in d shows the expected position for the first order diffraction spots for the two-layer ice on graphene/Pt(111), which has a lattice constant, a_{2D}, of 0.481 nm. For all experiments, the sample temperature during the LEED measurement was 20 K.

grown on clean Pt(111) at 145 K. (Cubic ice is metastable with respect to I_h, but is structurally very similar to I_h.[21]) Helium atom scattering[28] has shown that multilayer ice grown on Pt(111) under similar conditions has hexagonal symmetry, with $a_{I_c} = 0.452$ nm (i.e., consistent with bulk-terminated I_c or I_h). Figure 1d shows an example of the LEED pattern obtained for a 20 ML H_2O film grown on Pt(111). Similar patterns were obtained for 10 ML H_2O films and for 20 ML D_2O films. We find $a_{I_c} = 0.452 \pm 0.003$ nm for H_2O and D_2O ice on Pt(111) in excellent agreement with the expected value.[28] We also note that the lattice constant obtained from the LEED patterns for the graphene films ($a_{gr} = 0.246$ nm) grown on Pt(111) (see Figure 1a) agrees with previously reported values.[19,29]

For the ice films grown at 125 K on graphene/Pt(111) [e.g., b and c in Figure 1], the measured lattice constant ($a_{2D} = 0.481$ nm) suggests that the ice has an unusual bonding geometry. With tetrahedral bonding and this lattice constant, the oxygen−oxygen distance, r_{OO}, would be 0.294 nm, which is quite long compared to the typical values in ice.[21] However for a flat hexagonal 2 ML ice film (as discussed below), the observed lattice constant corresponds to $r_{OO} = 0.278$ nm, which is very close to the r_{OO} distance (0.275 nm) in I_h at low temperatures.[21]

The adsorption/desorption of rare gases can be a useful tool for characterizing the growth of thin water films on surfaces.[30,31] Its utility arises because the van der Waals interaction of a rare gas with water is often weaker than its interaction with the substrate. Therefore, the desorption peak for rare gas atoms desorbing from the bare substrate during TPD is easily distinguished from the peak corresponding to desorption from the water. The key point is that the area of the bare surface peak in TPD is proportional to the fraction of the surface that is not covered by the water film. Therefore, the TPD spectra allow one to asses the extent to which a given water film covers the substrate. For example, the inset to figure 2 shows several TPD spectra of ~1 ML Ar on graphene/Pt(111) covered with various amounts of water. The peak labeled W_c at ~42 K is due to Ar desorbing from graphene/Pt(111), whereas the peak at ~31 K (labeled W_{ice}) is due to Ar desorbing from the water films. As θ increases, the area of W_c decreases, whereas the area of W_{ice} increases.

Figure 2 shows the normalized area of W_c versus the amount of water adsorbed on the surface, θ, for both H_2O (circles) and D_2O (triangles) on graphene/Pt(111) at 125 K. For this data, the amount of water adsorbed on the graphene/Pt(111) as a function of the water dose has been calculated from water TPD spectra obtained after the Ar TPD spectra. Therefore, the data account for the changing water condensation coefficient versus water coverage. In Figure 2, the normalized area of W_c corresponds to the fraction of the surface not covered by ice, F_c. For both H_2O and D_2O, F_c decreases linearly for $\theta \lesssim 1.2$ ML, and the slope then gradually decreases for higher coverages.

(28) Braun, J.; Glebov, A.; Graham, A. P.; Menzel, A.; Toennies, J. P. *Phys. Rev. Lett.* **1998**, *80*, 2638.
(29) Hu, Z. P.; Ogletree, D. F.; Van Hove, M. A.; Somorjai, G. A. *Surf. Sci.* **1987**, *180*, 433.
(30) Kimmel, G. A.; Petrik, N. G.; Dohnálek, Z.; Kay, B. D. *Phys. Rev. Lett.* **2005**, *95*, 166102.
(31) Kimmel, G. A.; Petrik, N. G.; Dohnálek, Z.; Kay, B. D. *J. Chem. Phys.* **2007**, *126*, 114702.

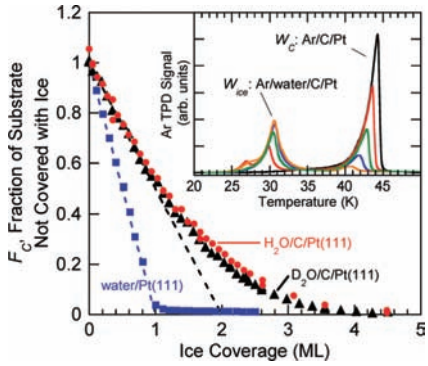

Figure 2. Fraction of substrate not covered with ice, F_c, versus water coverage. On Pt(111), the first water monolayer (D_2O or H_2O) wets the surface and F_c decreases with a slope of -1 (squares). On graphene/Pt(111), F_c initially decreases with a slope of -0.5 for both H_2O (circles) and D_2O (triangles). The water films were grown at 125 K. Inset: Ar TPD's for 0 ML (black line), 0.77 ML (red), 1.66 ML (green), 2.60 ML (blue), and 3.55 ML (orange) D_2O films on graphene/Pt(111).

The surface is completely covered by the water films for $\theta > 4$ ML. We have obtained similar results for deposition temperatures between ~100 and 130 K (depending on the water flux). Also shown in Figure 2 is F_c versus θ for D_2O grown on Pt(111) at 125 K (squares).[30] The slope of F_c versus θ is inversely related to the average thickness of the water films that are growing on the surface. For example, since the first layer of water (H_2O or D_2O) wets Pt(111),[30,31] F_c versus θ decreases with a slope of -1 until $\theta = 1$ ML. On graphene/Pt(111) in contrast, F_c initially decreases with a slope of -0.5 (black dashed line). Therefore, the average height of these ice films is two water layers.

From Figures 1 and 2, we conclude that water on graphene/Pt(111) initially grows in ice islands that azimuthally align with and wet the graphene. The ice has hexagonal symmetry, an average thickness of two layers, and a lattice constant that is 6.4% larger than I_c. Upon heating above ~135 K, we find that the two-layer ices dewet the graphene surface, and the RAIRS spectra after dewetting are similar to the spectrum for I_c (data not shown). Thus, the two-layer ices are metastable with respect to I_c and convert to nonwetting, 3D I_c crystallites upon annealing.

Motivated by the experimental results and previous (empirical) MD simulations of water films confined between hydrophobic walls,[7,9,10] we investigated two-layer ice films using ab initio MD. Panels a and b in Figure 3 show top and side views, respectively, of the time-averaged structure of a two-layer H_2O ice at 150 K. (Similar results were obtained for simulations at temperatures ranging from 25 to 150 K.) From above (Figure 3a), the water is bonded in the familiar hexagonal arrangement. However for the calculated two-layer ice, the lattice constant within the hexagonal sheets is $a_{2D} = 0.476$ nm, which agrees well with the experiments. The side view (Figure 3b) clearly demonstrates the planar character of this two-layer ice. The oxygen atoms lie in two planes separated by 0.285 nm (Figure 3d), whereas in I_h, the oxygen atoms in each hexagonal sheet lie in two distinct planes that are displaced by 0.091 nm from each other (i.e., they form a "bilayer"), and these bilayers are separated by 0.366 nm (Figure 3c).

In I_h, the upper half of the molecules in a bilayer are bound to the molecules in the bilayer above it, and the lower half are bound to the molecules in the bilayer below it (Figure 3c). However, for the two-layer ice films, every water molecule in a given layer is hydrogen-bonded to the molecule in the other layer. Around any hexagon, the molecules alternate between

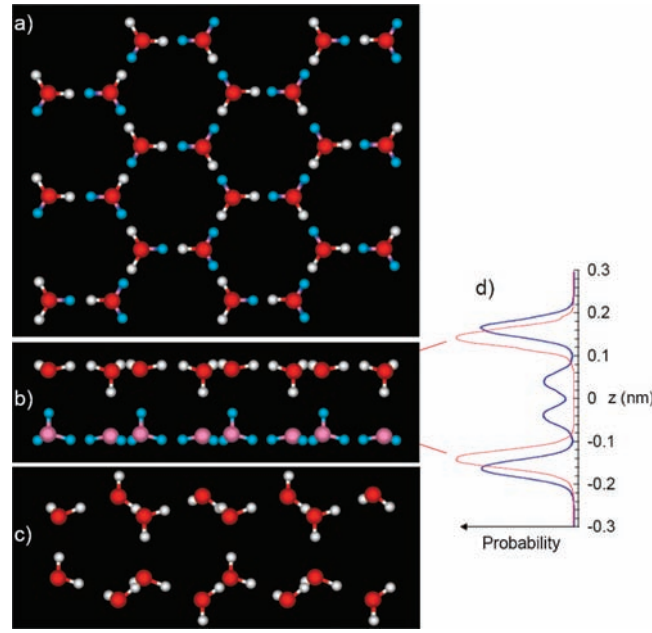

Figure 3. Calculated two-layer ice structure. (a, b) Average positions of the molecules in the two-layer ice for a 5 ps trajectory at 150 K. The white (blue) spheres represent hydrogen atoms in top (bottom) layer. Red (pink) spheres represent oxygen atoms in the top (bottom) layer. (a) Top view. The two-layer ice has hexagonal symmetry with a calculated lattice constant, a_{2D}, of 0.476 nm. (b) Side view showing the two flat layers of molecules with hydrogen bonds connecting the layers. (The hydrogen atoms in between the two layers, which appear close together in this view, are displaced laterally relative to each other in the plane perpendicular to the figure and are in fact separated by 0.29 nm.) (c) Side view of normal hexagonal ice. In I_h the oxygen atoms in the (0001) plane form puckered "bilayers". (d) In the two-layer ice, the oxygen atoms lie in two planes separated by 0.285 nm (red line), and the "in-plane" hydrogen atoms (blue line) are situated "outside" the oxygen atoms.

"bridging" molecules, which have one hydrogen pointing toward the other sheet, and "in-plane" molecules, whose hydrogens are both (nearly) in the plane and which is a hydrogen-bond acceptor for its counterpart in the other sheet. Therefore, three-quarters (one-quarter) of the hydrogen bonds are approximately parallel (perpendicular) to the hexagonal sheets.

Because the water molecules in the two-layer ice films are significantly distorted relative to the tetrahedral bonding found in I_h, we expect this to affect the molecular vibrations and the lattice dynamics. RAIRS is sensitive to the vibrations and librations (i.e., hindered rotations) of adsorbed water,[4,32] and therefore we have used it to further characterize the two-layer ice films. We also compare the experimental results to IR spectra calculated from the ab initio MD simulations.

The solid lines in Figure 4 show the experimental RAIRS spectra for several ice films on graphene/Pt(111). For these spectra, the absorbance was normalized by θ for each film to facilitate the comparison of various films with different water coverages. The solid red line shows the spectrum for a 35 ML H_2O film deposited at 145 K on graphene/Pt(111). This spectrum, which has its main peak in the OH-stretch region at 3220 cm^{-1}; a broad, weak peak in the υ_2 region at ~1650 cm^{-1}; another broad, weak band centered at 2250 cm^{-1}; and a peak centered at 890 cm^{-1} due to librations, is characteristic of I_c or I_h.[33] For 1.5 ML of H_2O deposited on graphene/Pt(111) (Figure

(32) Thiel, P. A.; Madey, T. E. *Surf. Sci. Rep.* **1987**, *7*, 211.

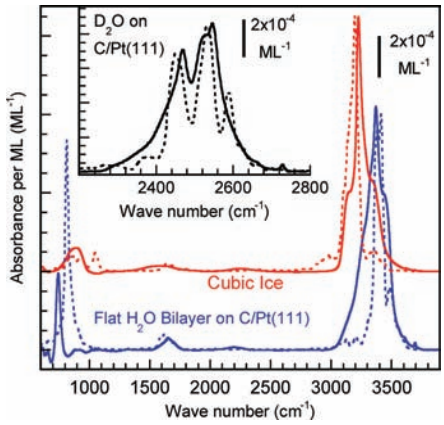

Figure 4. Experimental (solid lines) and theoretical (dashed lines) reflection−absorption infrared spectra (per monolayer) versus frequency for water films on graphene/Pt(111). The frequencies for the calculated spectra have all been scaled by 1.025 to facilitate comparison with the experimental results. For 1.5 ML H_2O on graphene/Pt(111) deposited at 125 K (solid blue line), the spectrum is blue-shifted relative to cubic ice (solid red line) in the OH-stretch region (∼3200−3500 cm^{-1}), and the librations (∼750 cm^{-1}) are red-shifted. The inset shows the IR spectra in the OD-stretch region for 0.75 ML D_2O deposited at 125 K.

4, solid blue line), the spectrum is quite different: 1) The spectrum is *blue-shifted* by ∼150 cm^{-1} in the OH-stretch region, with the peak of the adsorption at 3370 cm^{-1} and a shoulder at 3466 cm^{-1}. 2) In the ν_2 region, there is a weak feature at ∼1650 cm^{-1}, and 3) there is a librational band with a peak at ∼745 cm^{-1} that is *red-shifted* relative to I_c. RAIRS spectra very similar to this are also found for $0 < \theta \leq 2$ ML.

Figure 5a shows a series of RAIRS spectra in the OD-stretch region for 0.15 ML $\leq \theta \leq$ 2.1 ML. The spectra have two distinct peaks at 2470 and 2547 cm^{-1}, and a shoulder at 2525 cm^{-1}. As the coverage increases, the intensity of the spectra also increases. However, as shown in Figure 5b (which shows these same spectra normalized by the peak intensity at 2547 cm^{-1}), the shape of the spectra is independent of coverage for $\theta \leq 1.2$ ML, and shows only modest changes for 1.2 ML $< \theta \leq 2.1$ ML. To investigate the influence of a second hydrophobic interface, we have also measured the RAIRS spectra of two-layer ices that were subsequently capped with multilayer decane films. The spectra were similar to those in Figures 4 and 5, indicating that the structure of the "confined" two-layer ice film had not changed (data not shown).

The FTIR spectra in Figure 5 show that for $\theta <$ ∼1.2 ML, the structure of the water films does not depend on θ. These results, in conjunction with the results in Figures 2, suggest that for $\theta \lesssim 1.2$ ML, the water films grow in islands that are two layers thick where the local structure within the islands (shown in Figure 3) is independent of the water coverage. This is not too surprising because, at low coverages, it is likely that the islands grow independently. However, as the water coverage increases, the islands should begin to coalesce. At this point, the results suggest that some water begins to grow on top of the two-layer ice islands (perhaps at the domain boundaries between impinging islands), causing F_c versus θ to deviate from linearity (Figure 2) and the normalized FTIR spectra to change (Figure 5b). However, the two-layer ice islands continue to grow (i.e., F_c decreases), the films retain hexagonal symmetry with a lattice constant of 0.481 nm (Figure 1), and the changes in the FTIR spectra are modest. The growth of water films on

(33) Bertie, J. E.; Whalley, E. *J. Chem. Phys.* **1964**, *40*, 1637.

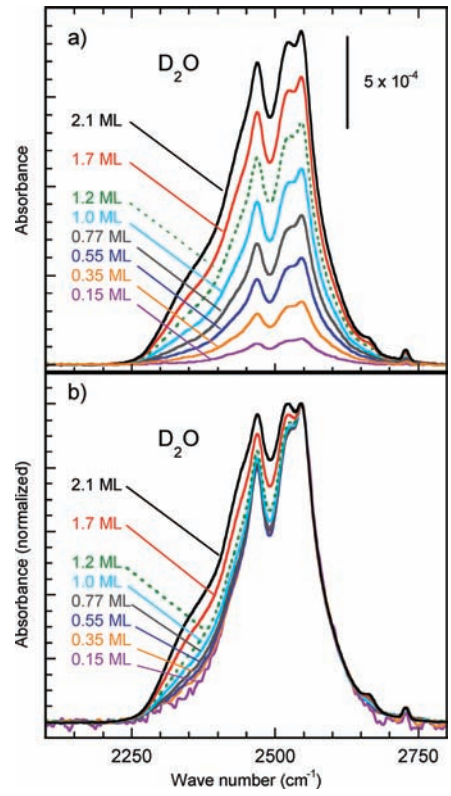

Figure 5. Reflection−absorption infrared spectra in the OD-stretch region of D_2O films grown at 125 K on graphene/Pt(111) for various D_2O coverages. (a) As the D_2O coverage increases, the intensity increases. (b) Peak normalized RAIRS spectra. For $\theta \leq 1.2$ ML, the normalized RAIRS spectra are nearly indistinguishable. For 1.2 ML $< \theta \leq 2.1$ ML, the relative intensity of lower frequency portion of the OD-stretch band increases slightly.

graphene/Pt(111) for larger coverages will be addressed in a future publication. Here, we are primarily interested in the structure of the water films for coverages where the two-layer islands are not interacting.

Figure 4 also shows the calculated IR spectra for I_c (dashed red line), and for two-layer crystalline ice films of H_2O (dashed blue line) and D_2O (inset, dashed black line) The spectra were calculated directly using the Fourier transform of the autocorrelation function of the total dipole moment from two independent 5 ps trajectories (10 ps for I_c) in the microcanonical ensemble. We find that the calculated frequencies are consistently a little smaller than the experimental values. Thus to facilitate comparison with experiment, all the calculated frequencies have been scaled by a factor of 1.025.[34] Furthermore, RAIRS is not sensitive to vibrations parallel to the surface due to the surface-dipole selection rule.[4,32] Therefore, to compare the calculated spectra with the experiments, the calculated spectra in Figure 4 show only the component normal to the surface.

The calculated IR spectra (Figure 4, dashed lines) capture all the salient features that are observed experimentally for the two-layer ice: (1) The OH (OD) stretch band is blue-shifted

(34) Since we will be comparing the relative shifts in the RAIRS spectra between I_c and the two-layer ices, scaling the calculated frequencies by 2.5% will not change the conclusions. Furthermore, considering the inherent uncertainties in DFT associated exchange and correlation, and that the experimental ice films were grown on a graphene film while the simulated films were not, the small discrepancy between the calculated and observed frequencies is not surprising.

relative to I_c. (2) There is a broad, weak band in the ν_2 region of the spectra ($\sim$1650 cm^{-1}) that is not appreciably shifted. (3) There is a relatively intense librational mode at low frequencies that is red-shifted relative to I_c. The similarities between the experimental and calculated IR spectra reported here confirm that we have grown two-layer crystalline ice films on graphene/Pt(111) with the structure shown in Figure 3. The results also suggest that the role of the graphene is simply to provide a flat, hydrophobic template for assembling the planar, two-layer ice. In particular, the details of the water−graphene interaction do not appear to be important in determining the structure of the ice beyond the experimentally observed azimuthal ordering (see Figure 1). As a result, the two-layer ices observed here might also form on other flat hydrophobic substrates such as graphite and Au(111).

The structure of the two-layer ice films (Figure 3) reflects the fact that it is energetically costly to have broken hydrogen bonds. Because the water-graphene (water-vacuum) interaction is weak (zero), the water molecules adopt a structure with a strained bonding geometry, but one which has all the water molecules bonded to four neighbors.[35] The systematic shifts in the IR spectra of the two-layer ices relative to I_c (see Figure 4) are easily explained in terms of weakened hydrogen bonds in the two-layer ice resulting from the strained bonding: The blue shift in the OH stretch region is due to the weaker hydrogen bonds formed by the "bridging" water molecules in the two-layer ice. Our calculated IR spectra also predict a blue-shift in the OH stretch region for vibrations parallel to the surface (data not shown) due to the weakened hydrogen bonds within each sheet of the two-layer ice. However, for hydrogen bonds within each sheet, the bonds are less strained ($\theta_{OOO} = 120°$ versus 90°), so the blue shift is smaller. The weaker hydrogen bonding also gives rise to more pronounced librations which are red-shifted relative to I_c. Interestingly, the IR spectra of water confined in carbon nanotubes showed a blue-shifted peak in the OH-stretch region that was also attributed to weakened hydrogen bonding arising from the strained bonding geometry.[11]

The structure of the two-layer ice explains why it readily forms on graphene even though it is metastable with respect to bulk ice. The number of broken hydrogen bonds per water molecule is smaller for a two-layer ice cluster than it is for a three-dimensional (3D) I_h cluster of the same size.[36] Thus for the small clusters that initially grow on the graphene, the total free energy of the two-layer ice is lower than a 3D ice crystallite of the same size,[36] and hence their formation is favored. Once nucleated, the structure of the two-layer ice clusters also facilitates their subsequent growth: Since all the water molecules in the two-layer ice clusters are fully coordinated except for those on the perimeter, water initially adsorbing on top of the cluster will be weakly bound until it diffuses to the edge where it can be readily incorporated into the growing cluster. Finally, because the ideal two-layer ice has no broken bonds, the surface free energy is low, which explains why these ice films wet the hydrophobic graphene surface. (We are currently investigating the structure of the ice films for coverages greater than 2 ML and the results will be presented elsewhere.)

An important question is the range of temperatures over which the two-layer ice is metastable. As discussed above, we find that the unconfined two-layer ice transforms to 3D nonwetting I_c crystallites upon heating above $\sim$135 K. However, MD simulations predict that under external pressure, confined two-layer ices can be stable even at room temperature.[7] Furthermore, Jinesh and Frenken[37] have recently presented experimental evidence for the formation of an ice film (of unknown structure and thickness) at room temperature between a graphite surface and the tungsten tip of a high-resolution friction force microscope.

An early MD simulation of liquid water confined between hydrophobic walls predicted that the structure near the interface results from the tendency to maximize the packing density of the molecules in the first layer, while simultaneously maximizing the number of hydrogen bonds formed by the molecules in that layer.[5] However, because the water molecules in those simulations were rigid, fulfilling these conditions led to a predominantly bulk icelike structure where approximately half the molecules in the first layer had only three hydrogen bonds. The results presented here suggest that for real water molecules where the bonding geometry is flexible, maximizing the packing density in the first layer does not necessarily lead to broken hydrogen bonds. Instead, the molecules can adopt a nontetrahedral bonding geometry.

Recent ab initio MD simulations of two-layer liquid D_2O confined between graphene walls at near ambient temperatures[8,38] showed interesting similarities to the results presented here. In particular, the shifts in the IR spectra for the confined liquid water relative to bulk water were similar to the changes observed here for two-layer ice relative to bulk ice.[38] Furthermore, the second most common orientation for the hydrogen bonds was pointing away from the surface. (The majority of the hydrogen bonds were approximately parallel to the surface, as expected.) Although the simulation results for two-layer liquid and crystalline ices are similar, the blue-shift in the OD stretch for liquid D_2O was attributed to interactions between the D_2O and the graphene.[38] Because we have no dangling OH's/OD's or graphene walls, this cannot be the source of the blue shift in our simulations. Instead, the experiments and calculations presented herein support the idea that the blue shift in the water OH-stretch results from the formation of weaker hydrogen bonding arrangements. Comparison of our results with the simulations of confined liquid water suggest that the binding motifs observed in the planar, two-layer ice films at low temperature might also play a role in the structure of liquid water near hydrophobic surfaces. More research is needed to understand under what conditions and to what extent these strained hydrogen-bonding structures occur at the interfaces of liquid water with hydrophobic surfaces.

4. Summary

In summary, we report the observation of two-layer crystalline ice films grown in ultrahigh vacuum on a planar, hydrophobic substrate. These two-layer ices, which are metastable with respect to three-dimensional hexagonal ice, have an interesting nontetrahedral bonding geometry. In each layer of the ice, the water molecules are arranged in planar, hexagonal units (i.e.,

(35) In Figures 4 and 5, the dangling OH and OD peaks at 3696 and 2730 cm^{-1}, respectively, are small, suggesting that there are relatively few broken hydrogen bonds in the films. However, because of the small dynamic dipole moment for the dangling OH's (OD's) compared to the OH's (OD's) involved in hydrogen-bonding, the IR intensity of these dangling OH's (OD's) is typically small and a quantitative assessment of the number of broken hydrogen bonds using this data is difficult. This issue will be addressed in detail in a future publication.

(36) Tanaka, H.; Yamamoto, R.; Koga, K.; Zeng, X. C. *Chem. Phys. Lett.* **1999**, *304*, 378.

(37) Jinesh, K. B.; Frenken, J. W. M. *Phys. Rev. Lett.* **2008**, *101*, 036101.

(38) Sharma, M.; Donadio, D.; Schwegler, E.; Galli, G. *Nano Lett.* **2008**, *8*, 2959.

$\theta_{OOO} = 120°$) with a lattice constant of 0.481 nm, and the two water layers are stacked directly on top of each other. This arrangement maximizes the number of hydrogen bonds in the ice film. Since there are also no dangling OH's or lone pair electrons on either surface of the film, the interaction of the ice with the hydrophobic substrate is weak. The results reported here add support to previous molecular dynamics simulations that predicted the formation of two-layer ices in confined geometries.

Acknowledgment. This work was supported by the U.S. Department of Energy (DOE), Office of Basic Energy Sciences, Chemical Sciences Division. Experiments and calculations (using NWice) were performed in the W. R. Wiley Environmental Molecular Sciences Laboratory at Pacific Northwest National Laboratory, which is a National Scientific User Facility operated for DOE, Office of Biological and Environmental Research, by Battelle Memorial Institute under Contract DE-AC06-76RLO 1830. M.B. gratefully acknowledges partial financial support by Deutsche Forschungsgemeinschaft (DFG) and by Fonds der Chemischen Industrie (FCI) through grants to Dominik Marx (Bochum).

JA904708F